C.P. No. 456
(20,677)
A.R.C. Technical Report

C.P. No. 456
(20,677)
A.R.C. Technical Report

MINISTRY OF SUPPLY

AERONAUTICAL RESEARCH COUNCIL

CURRENT PAPERS

Transonic Flow over Two-Dimensional Round-Nosed Aerofoils

by

D. G. Randall, B.Sc.

LONDON: HER MAJESTY'S STATIONERY OFFICE

1959

FOUR SHILLINGS NET

C.P. No.456

U.D.C. No. 533.6.011.35 : 533.69.048.2 : 533.692

Technical Note No. Aero.2579

September, 1958.

ROYAL AIRCRAFT ESTABLISHMENT

TRANSONIC FLOW OVER TWO-DIMENSIONAL ROUND-NOSED AEROFOILS

by

D.G. Randall, B.Sc.

SUMMARY

A technique developed by Spreiter and Alksne for determining the pressure distribution over a two-dimensional sharp-nosed aerofoil moving at a speed in the transonic range is extended to the case of a round-nosed aerofoil. If there are no shocks before the trailing edge, Sinnott's method can be used for calculating the pressure distribution over the rear part of the wing. The method is applicable to a round-nosed aerofoil at incidence.

LIST OF CONTENTS

ILLUSTRATIONS - Figs.1-9

LIST OF ILLUSTRATIONS

---

1 INTRODUCTION

The determination of the transonic flow over an arbitrary two-dimensional aerofoil has long been one of the most exasperating unsolved problems of aerodynamics. The partial differential equation for the velocity potential is simple, the boundary conditions can be set up without difficulty, and the problem is of considerable practical importance. In spite of all this the results obtained were, until recently, scanty.

Two main methods had been tried, the hodograph method and the integral equation method. In the first of these the (non-linear) differential equations of motion are transformed so that the velocities become the independent variables while the spatial coordinates become the dependent variables. The transformed equations are linear and solutions of them can be built up by superposition. A description of this theory forms the major part of Guderley's interesting book[1], which also contains a comprehensive list of references. The greatest difficulty in the use of the hodograph method is that the boundaries in the physical plane, along which data are prescribed, are, in general, unknown in the hodograph plane. This has restricted the use of the hodograph method to studies of transonic flow over wedges and flat plates; there is no lack of such studies. An extension to flow over curved surfaces might be possible by a "trial and error" process, but such a process would be most laborious.

The integral equation method originated with Oswatitsch[2] and was elaborated by Gullstrand[3]. In this method, (almost a method of despair), the differential equations of motion are transformed into a (non-linear) integral equation, some approximations are made to the integrand, a guess at the velocity distribution over the aerofoil is made, and a solution is obtained by iteration. Another elaboration of Oswatitsch's method was given by Spreiter and Alksne[4]. As in Gullstrand's work[3] the technique permits the calculation of the position and strength of shock waves on the aerofoil. Agreement with the few experimental results available is unexciting. The integral equation method is preferable to the hodograph method since curved profiles can be treated, but it is tedious to apply and the effects of the approximations introduced are not easy to estimate.

A third approach to the solution of the problem is also due to Oswatitsch. Some work by Behrbohm[5] is based on a suggestion of Oswatitsch that a factor of a term in the differential equations be taken as an undetermined constant. The equations then become linear and a solution is obtained with one arbitrary constant. A paper by Oswatitsch and Keune[6] contains a method for determining this constant in the axisymmetric case. The examples included there show that Oswatitsch's suggestion can lead to useful results. A remarkable paper by Spreiter and Alksne[7] has recently appeared which is based on an ingenious refinement of Oswatitsch's suggestion. The method described there leads to a simple analytical expression for the pressure distribution over an arbitrary profile, and the results are in striking agreement with experiment.

The present note briefly describes the work of Spreiter and Alksne[7], and extends it to round-nosed profiles and profiles at incidence. The methods are applied to a profile which has been extensively investigated by Holder and Cash[8].

2 THE WORK OF SPREITER AND ALKSNE

A brief description only is given here: the interested reader is referred to the original paper[7] for a full treatment.

The problem is to determine the steady transonic flow over a two-dimensional, thin, symmetrical profile. Cartesian coordinates, x and y, are introduced, with origin at the nose of the profile; the line of symmetry of the profile is part of the x axis, and the y axis is normal to this. The x direction coincides with the free stream direction. The speed of the free stream is U_∞ and the Mach number is M_∞. Even when shock waves are present the flow may be assumed to be irrotational; since the aerofoil is thin, a disturbance velocity potential, ϕ, may be introduced, such that

$$\text{x velocity} = U_\infty (1 + \phi_x) = U_\infty (1 + u) \qquad (1a)$$

while

$$\text{y velocity} = U_\infty \phi_y = U_\infty v \quad , \qquad (1b)$$

the suffixes denoting partial derivatives. u and v may be termed "incremental velocities". ϕ satisfies the following non-linear second-order partial differential equation:

$$\phi_{yy} - (\gamma + 1) M_\infty^2 \phi_x \phi_{xx} = (M_\infty^2 - 1) \phi_{xx} \quad , \qquad (2)$$

γ being the ratio of the specific heats of the fluid. The boundary conditions that the solution of (2) must satisfy are that the incremental velocities vanish at infinity and that the given profile be a streamline. If the equation of the profile is:

$$y = \tau h (x) \qquad (3)$$

where h is of order one and τ is a constant of the order of the thickness chord ratio of the profile, the boundary condition may be written, in simplified form:

$$y = 0, \qquad \phi_y = \tau h' (x) \qquad (4)$$

the prime denoting differentiation. The equations giving the changes in the incremental velocities across a shock also take on a simplified form in transonic flow[1]; since they are not needed in this note, there is no point in giving them here.

(2) may be written

$$\phi_{yy} - \lambda \phi_x = (M_\infty^2 - 1) \phi_{xx} + \left[(\gamma + 1) M_\infty^2 \phi_{xx} - \lambda \right] \phi_x \equiv f(x,y) \qquad (5)$$

where λ is an unspecified constant. The right hand side is regarded as a given function of x and y, f(x,y), although it is a known function only when (2) has been solved. (5) can be solved by the use of Green's theorem, the solution being

$$\phi(x,y) = -\frac{1}{\lambda} \int_0^x \left(\sigma \Delta \frac{\partial \phi}{\partial \eta} - \frac{\partial \sigma}{\partial \eta} \Delta \phi \right)_{\eta=0} d\xi - \frac{1}{\lambda} \int_{-\infty}^{\infty} \int_{-\infty}^{x} \sigma f(\xi,\eta) \, d\xi \, d\eta \qquad (6)$$

for positive λ, and

$$\phi(x,y) = \frac{1}{\lambda}\int_0^x \left(\sigma \Delta\frac{\partial\phi}{\partial\eta} - \frac{\partial\sigma}{\partial\eta}\Delta\phi\right)_{\eta=0} d\xi + \frac{1}{\lambda}\int_{-\infty}^{\infty}\int_{-\infty}^{x} \sigma f(\xi,\eta)\, d\xi\, d\eta \qquad (7)$$

for negative λ. ξ and η are running coordinates corresponding to x and y respectively. σ is the "unit heat source",

$$\sigma = \left[\frac{\lambda}{4\pi(x-\xi)}\right]^{\frac{1}{2}} e^{\left[-\frac{\lambda(y-\eta)^2}{4(x-\xi)}\right]} \quad \text{if} \quad \frac{\lambda}{x-\xi} > 0 \qquad (8a)$$

$$\sigma = 0 \quad \text{if} \quad \frac{\lambda}{x-\xi} < 0 \qquad (8b)$$

$(\Delta\phi)_{\eta=0}$ and $\left(\Delta\frac{\partial\phi}{\partial\eta}\right)_{\eta=0}$ are defined by

$$(\Delta\phi)_{\eta=0} = \phi_u - \phi_\ell \qquad (9a)$$

and

$$\left(\Delta\frac{\partial\phi}{\partial\eta}\right)_{\eta=0} = \left(\frac{\partial\phi}{\partial\eta}\right)_u - \left(\frac{\partial\phi}{\partial\eta}\right)_\ell \qquad (9b)$$

suffixes u and ℓ referring to conditions on the upper and lower sides respectively of the wing and wake. (6) and (7) are valid if either shock waves are absent from the region defined by the limits of the double integral or the shock waves present in this region are parallel to the y axis. For a symmetrical profile (9a) shows that $(\Delta\phi)_{\eta=0}$ is zero while, from (4) and (9b),

$$\left(\Delta\frac{\partial\phi}{\partial\eta}\right)_{\eta=0} = 2\tau h'(\xi) \quad .$$

(6), (7), (8a) and (8b) now lead to

$$u(x,0) = \left(\frac{\partial\phi}{\partial x}\right)_{y=0} = -\frac{\tau}{(\pi\lambda)^{\frac{1}{2}}}\frac{d}{dx}\int_0^x \frac{h'(\xi)\, d\xi}{(x-\xi)^{\frac{1}{2}}} -$$

$$-\frac{1}{\lambda}\frac{d}{dx}\left\{\int_{-\infty}^{\infty}\int_{-\infty}^{x}\sigma f\, d\xi\, d\eta\right\}_{y=0} \qquad (10)$$

for $\lambda > 0$

and

$$u(x,0) = \left(\frac{\partial \phi}{\partial x}\right)_{y=0} = -\frac{\tau}{(-\pi\lambda)^{\frac{1}{2}}} \frac{d}{dx} \int_x^c \frac{h'(\xi)\, d\xi}{(x-\xi)^{\frac{1}{2}}} +$$

$$+ \frac{1}{\lambda} \frac{d}{dx} \left\{ \int_{-\infty}^{\infty} \int_x^{\infty} \sigma f \, d\xi \, d\eta \right\}_{y=0} \qquad (11)$$

for $\lambda < 0$,

c being the aerofoil chord.

(10) and (11) have been derived from (2) without further approximations (other than a restriction on the orientation of shock waves). λ is an unspecified constant. Spreiter and Alksne[7] now replace this constant by a function of x,

$$(\gamma + 1) M_\infty^2 [\phi_{xx}]_{y=0} \quad ,$$

i.e. by $$(\gamma + 1) M_\infty^2 u'(x,0) \quad .$$

They further assume that, in the integrand of the double integral,

$$f(\xi,\eta) \equiv (M_\infty^2 - 1)\, \phi_{\xi\xi} + [(\gamma + 1) M_\infty^2 \phi_{\xi\xi} - \lambda]\, \phi_\xi$$

$$= (M_\infty^2 - 1)\, \phi_{\xi\xi} + (\gamma + 1) M_\infty^2 [\phi_{\xi\xi} - (\phi_{xx})_{y=0}]\, \phi_\xi$$

$$= (M_\infty^2 - 1)\, \phi_{\xi\xi} = (M_\infty^2 - 1)(\phi_{xx})_{y=0}$$

$$= (M_\infty^2 - 1)\, u(x,0)$$

In other words they assume that $\phi_{\xi\xi}$ is equal to $(\phi_{xx})_{y=0}$ everywhere. Abbreviating u(x,0) to u, (10) and (11) become

$$u = -\frac{\tau}{[(\gamma + 1)\, \pi M_\infty^2 u']^{\frac{1}{2}}} \frac{d}{dx} \int_0^x \frac{h'(\xi)\, d\xi}{(x-\xi)^{\frac{1}{2}}} + \frac{(1 - M_\infty^2)}{(\gamma + 1) M_\infty^2} \qquad (12)$$

for positive u', and

$$u = \frac{\tau}{[-(\gamma + 1)\, \pi M_\infty^2 u']^{\frac{1}{2}}} \frac{d}{dx} \int_x^c \frac{h'(\xi)\, d\xi}{(x-\xi)^{\frac{1}{2}}} + \frac{(1 - M_\infty^2)}{(\gamma + 1) M_\infty^2} \qquad (13)$$

for negative u'. These approximations are discussed in detail in the appendix to ref.7; the excellent agreement with experiment is sufficient justification for making them.

(12) and (13) are non-linear ordinary differential equations for u on the aerofoil surface. (13) will not be considered further in this section; it can be treated in the same way as (12). The solution of (12) is

$$u = \frac{1 - M_\infty^2}{(\gamma + 1) M_\infty^2} + \left(\frac{3}{\pi}\right)^{1/3} \frac{\tau^{2/3}}{(\gamma + 1)^{1/3} M_\infty^{2/3}} \left[\int_{x^*}^{x} \left\{ \frac{d}{d\xi_1} \int_0^{\xi_1} \frac{h'(\xi_2)\, d\xi_2}{(\xi_1 - \xi_2)^{\frac{1}{2}}} \right\}^2 d\xi_1 \right]^{1/3} \qquad (14)$$

with x^* an undetermined constant. When

$$x = x^* \quad ,$$

u becomes

$$\frac{1 - M_\infty^2}{(\gamma + 1) M_\infty^2}$$

which is the value of u at the sonic point on the usual transonic approximation. (14) gives an infinite value for u' at $x = x^*$ unless x^* is chosen to be the value of x for which

$$\frac{d}{dx} \int_0^x \frac{h'(\xi)\, d\xi}{(x - \xi)^{\frac{1}{2}}} = 0 \quad . \qquad (15)$$

(14) can be used only so long as u' is positive. The above derivation of (12), where u' must be positive, and (13), where u' must be negative, shows that there is no possibility of overcoming this restriction.

The factor

$$\frac{\tau^{2/3}}{(\gamma + 1)^{1/3} M_\infty^{2/3}}$$

outside the square brackets in (14) means that the transonic similarity rules[9] hold for this solution. In addition, when (14) is used to find the variation of local Mach number with x it is found that, approximately, the variation is independent of M_∞. This phenomenon, which has been observed in experiment and has been commented on before[10], is picturesquely named the "Mach number freeze".

The biconvex aerofoil provides an interesting example. The equation of this profile is

$$y = 2\tau x \left(1 - \frac{x}{c}\right)$$

τ being the thickness chord ratio. The location of the sonic point comes from solving (15); hence

$$x^* = \frac{c}{4}$$

(14) leads to the following expression for u

$$u = \frac{1 - M_\infty^2}{(\gamma + 1) M_\infty^2} + \left(\frac{12}{\pi}\right)^{1/3} \frac{\tau^{2/3}}{(\gamma + 1)^{1/3} M_\infty^{2/3}} \left[\log\left(\frac{4x}{c}\right) - 8\frac{x}{c} + 8\left(\frac{x}{c}\right)^2 + \frac{3}{2}\right]^{1/3} \qquad (16)$$

This result is shown in ref.7 to compare very well with experiment.

Spreiter and Alksne[7] describe another technique for the solution of (2) which applies when the flow is either subsonic everywhere or supersonic everywhere. The function which is regarded first as a constant and then as a function of x only is now

$$(\gamma + 1) M_\infty^2 \phi_x \quad .$$

Applied to supersonic flows this approach leads to the differential equation

$$u' = -\frac{\tau}{[(M_\infty^2 - 1) + (\gamma + 1) M_\infty^2 u]^{\frac{1}{2}}} h'' \quad .$$

On integration this gives

$$u = \frac{1 - M_\infty^2}{(\gamma + 1) M_\infty^2} + \frac{1}{(\gamma+1) M_\infty^2} \left\{ [(\gamma+1) M_\infty^2 u_o - (M_\infty^2 - 1)]^{3/2} + \frac{3}{2} \tau (\gamma+1) M_\infty^2 (h_o' - h') \right\}^{2/3} \qquad (17)$$

where u_o and h_o' are values of u and h supposed given at a point $x = x_o$. (17) is, in fact, the transonic approximation to the result obtained by simple wave theory; it will be required in this note at a later stage.

3 EXTENSION TO ROUND-NOSED PROFILES

Because of the existence of the "Mach number freeze", flows with a free stream Mach number of unity only will be discussed in the rest of this note: (14) becomes:

$$u = \left(\frac{3}{\pi}\right)^{1/3} \frac{\tau^{2/3}}{(\gamma+1)^{1/3}} \left[\int_{x^*}^{x} \left\{ \frac{d}{d\xi_1} \int_{0}^{\xi_1} \frac{h'(\xi_2)\, d\xi_2}{(\xi_1 - \xi_2)^{\frac{1}{2}}} \right\}^2 d\xi_1 \right]^{1/3} \qquad (18)$$

Spreiter and Alksne[7] considered sharp-nosed profiles only, and for these x^*, the position of the sonic point on the aerofoil, is given by (15). The pressure distribution can then be obtained from (18). The problem of transonic flow over a symmetrical round-nosed profile is the subject of this section.

The difficulty arising when the method of section 2 is applied to a round-nosed profile can be seen by considering the profile whose equation is:

$$y = \tau \left(\frac{x}{c}\right)^{\frac{1}{2}} (c - x) \quad ; \qquad (19)$$

it has a sharp trailing edge and a maximum thickness of

$$\frac{4}{9}\sqrt{3}\, \tau\, c$$

at $x = \frac{1}{3} c$.

From (3)

$$2h'(x) = \left(\frac{c}{x}\right)^{\frac{1}{2}} - 3\left(\frac{x}{c}\right)^{\frac{1}{2}} .$$

The inner integral of (18) becomes

$$\frac{\pi}{2} c^{\frac{1}{2}} - \frac{3\pi}{4} \frac{\xi_1}{c^{\frac{1}{2}}}$$

and the differential coefficient of this is

$$-\frac{3\pi}{4c^{\frac{1}{2}}} .$$

The left hand side of (15) is, therefore

$$-\frac{3\pi}{4c^{\frac{1}{2}}} ,$$

and this equation no longer gives a value for the position of the sonic point. (18) becomes

$$u = \frac{3}{2}\left(\frac{\pi}{2}\right)^{1/3} \frac{\tau^{2/3}}{(\gamma+1)^{1/3}} \left[\left(\frac{x}{c}\right) - \left(\frac{x^*}{c}\right)\right]^{1/3} \quad . \qquad (20)$$

Although (15) has failed to provide a value for x^* it is shown in the next section that it does give a value for x^* when the incidence is not zero. As the incidence tends to zero so does x^*; hence, x^* in (20) is taken as zero. It is known[8] that, for some round-nosed aerofoils, the sonic point is, in fact, very close to the leading edge; in fact, profiles whose sonic point is not close to the leading edge are not universally in favour. The method of Spreiter and Alksne[7] applied to sharp-nosed aerofoils also breaks down near the leading edge ((16) shows that u has a logarithmic infinity there). It is, therefore, likely that having the sonic point, for round-nosed aerofoils, at the leading edge will not make the results any less useful than those obtained in ref.7. (20) becomes

$$u = \frac{3}{2}\left(\frac{\pi}{2}\right)^{1/3} \frac{\tau^{2/3}}{(\gamma+1)^{1/3}} \left(\frac{x}{c}\right)^{1/3} \quad .$$

The method described in section 2 cannot always be extended so easily to round-nosed profiles. The following equation describes a quite unexceptionable profile.

$$y = \tau\, c^{\frac{1}{2}}\, x^{\frac{1}{2}} \left[1 - \left(\frac{x}{c}\right)^{\frac{1}{2}}\right] \quad ;$$

it has a sharp trailing edge and a maximum thickness of $\frac{\tau c}{2}$ at $x = \frac{1}{4}c$. For this profile, using (18),

$$u = 2\left(\frac{3}{\pi}\right)^{1/3} \frac{\tau^{2/3}}{(\gamma+1)^{1/3}} \left(\log \frac{x}{x^*}\right)^{1/3} \quad , \qquad (21)$$

(15) again failing to provide a value for x^*. It is not possible to put x^* equal to zero in (21) and there is no obvious method for obtaining a plausible value for x^*. Hence, profiles whose expansion about $x = 0$ contains terms in both $x^{\frac{1}{2}}$ and x cannot yet be treated by the simple method discussed in this note. However, such profiles usually have undesirable features in the pressure distribution near the leading edge.

The above extension of the method of section 2 to round-nosed aerofoils is now applied to a profile, NPL.491, which has been investigated experimentally by Holder and Cash[8]. This profile has the equation

$$y = (c' - x)\left[1 - \left(\frac{c'-x}{c'+s}\right)^9\right] \tanh\left\{2\left[\left(\frac{x+s}{s}\right)^2 - 1\right]\right\}^{\frac{1}{2}} \tan\frac{\theta}{2} \qquad (22)$$

c' and s are equal to 9.409 inches and 0.341 inches respectively, and θ is 3.024°. The chord of the aerofoil is 9 inches, so that the profile is not closed at the rear end. Reasons for the choice of this profile are given in ref.8; it has a thickness chord ratio of 0.0418 and its maximum thickness occurs at $x = 0.209\ c$. Near the leading edge, from (22),

$$\frac{dy}{dx} = 0.0380 \left(\frac{c}{x}\right)^{\frac{1}{2}} \left[1 - 20.3 \left(\frac{x}{c}\right) + \ldots\right] \quad .$$

The factor of 20.3 is much too large for a "small disturbance" theory and so the profile has been slightly modified. Fig.1 shows the actual values of

$$\left(\frac{x}{c}\right)^{\frac{1}{2}} \frac{dy}{dx}$$

(full line) and the modification made (dashed line). The modification is confined to a region near the leading edge, where the method described here breaks down anyway. Even there, the difference between the two curves of Fig.1 is not excessive.

(18), with x^* put equal to zero, has been used to calculate the pressure distribution from $\frac{x}{c} = 0$ to $\frac{x}{c} = 0.4$, and the result is plotted in Fig.3 (full line). In this figure values of $\frac{p}{p_o}$, where p is static pressure and p_o stagnation pressure, are plotted against $\frac{x}{c}$. The formula for $\frac{p}{p_o}$ in terms of u (the free stream Mach number being one) is, neglecting squares and higher powers of the incremental velocities,

$$\frac{p}{p_o} = \left(\frac{2}{\gamma + 1}\right)^{\frac{\gamma}{\gamma-1}} (1 - \gamma u) = 0.528\ (1 - 1.4\ u)$$

$\frac{p}{p_o}$ depends on local Mach number only, the free stream Mach number not appearing explicitly; 0.528 is the value of $\frac{p}{p_o}$ at the sonic point. The numbers come from putting $\gamma = 1.4$, this value being used in all the numerical calculations. Also shown in Fig.3 are some of the experimental results obtained by Holder and Cash[8]. There is fair agreement with experiment. The sonic point is shown experimentally[8] to be at $x = 0.018\ c$; if this value is chosen for x^* instead of zero, u at $x = 0.1\ c$ differs by 5% from the value first obtained. The difference in $\frac{p}{p_o}$ is less than 1%.

The profile is one in which u passes through a maximum and, as has been mentioned already, the technique fails when $u' = 0$. Hence, (18) cannot be used beyond the point of maximum u; in fact, its value becomes doubtful at some point before this. To obtain an estimate of the pressure distribution over the whole profile, Sinnott's method[10] has been used. This method, which applies also to profiles at incidence, assumes that the flow quantities are known at the "crest" of the profile, i.e. at the point where y has its maximum value. Simple wave theory is used to obtain a first approximation for the quantities over that part of the profile downstream of the crest, (17)

being the appropriate equation. This approximation gives pressures which are too low, since it neglects the compression waves resulting from reflections at the sonic line. An estimate of the latter effect can be obtained by considering the flow at sonic speed over a double wedge, the solution of which is known[11]. Simple wave theory predicts that all the flow quantities are constant from the crest onwards, in particular, that ω, the Prandtl-Meyer angle, is constant. In Fig.2, $\Delta\omega$ (the difference between the true value of ω and the value of ω on simple wave theory) divided by the value of this quantity at the trailing edge is plotted against t, where

$$t = \frac{x - x_m}{c - x_m} \quad ,$$

x_m being the value of x at the crest. The same quantity is plotted for the two profiles

$$y = 2\tau c \left[\left(\frac{x}{c}\right)^{\frac{1}{2}} - \left(\frac{x}{c}\right)^{3/2} \right] \quad ,$$

and

$$y = 2\tau x \left(1 - \frac{x}{c}\right) \quad .$$

(17) and (18) have been used to obtain these two curves. Fig.2 suggests that the distribution of

$$\frac{\Delta\omega}{(\Delta\omega)_{t.e.}}$$

against t for the double wedge can be used for any profile. All that remains is to obtain an estimate for the true value of ω at the trailing edge, so that $(\Delta\omega)_{t.e.}$ can be determined. A result due to Holder[12] provides the required estimate; it states that the flow quantities at the trailing edge are such that, when the flow is deflected by an oblique shock through an angle corresponding to the slope at the trailing edge, the downstream Mach number is 1.08. This result gives a good approximation even when the profile is at incidence. The procedure recommended by Sinnott[10] is, therefore, to obtain ω downstream from the crest by simple wave theory, to obtain the true value of ω at the trailing edge by Holder's result[12], and then to use the curve in Fig.2 corresponding to the double wedge in order to correct the results of simple wave theory. This procedure gives the dashed curve in Fig.3; the agreement with experiment over most of the profile is satisfactory.

4 PROFILES AT INCIDENCE

Since (5) is a linear equation, lifting and non-lifting effects can be considered separately. In this section lifting effects are considered.

$$\left(\Delta \frac{\partial\phi}{\partial\eta}\right)_{\eta=0}$$

is zero and

$$(\Delta\phi)_{\eta=0}$$

is the integral of the loading from the leading edge to ξ (apart from a constant factor). For brevity $(\Delta\phi)_{\eta=0}$ is written as $g(\xi)$. (6) becomes

$$\phi(x,y) = \frac{1}{\lambda}\int_0^x g(\xi)\left(\frac{\partial\sigma}{\partial\eta}\right)_{\eta=0} d\xi - \frac{1}{\lambda}\int_{-\infty}^{\infty}\int_{-\infty}^{x} \sigma\, f(\xi,\eta)\, d\xi\, d\eta \qquad (23)$$

Differentiating (23) with respect to y and putting y = 0 leads to an integral equation for $g(\xi)$, (since $\left(\frac{\partial\phi}{\partial y}\right)_{y=0}$ is known from the aerofoil geometry). This integral equation can be solved without difficulty, and $u(x,0)$ is obtained by differentiating $g(x)$. The result is precisely the same as (12), with $h'(\xi)$ being the slope of the profile at ξ (the slopes on the upper and lower surfaces are now the same since the aerofoil is assumed to have no thickness). There is no need to give the details of the preceding mathematics, because the following argument shows that the result must be true. (5) is a parabolic equation and, for positive λ, the influence of a disturbance at a point can be felt downstream only of that point. It follows that the flow over the upper surface is independent of the lower surface and vice versa. Hence, the flow over the upper (or lower) surface can be determined by regarding it as the upper (or lower) surface of a symmetrical profile. This means that (14) can be used to obtain the flow over the upper surface of any profile (provided that $\tau\, h'(\xi)$ is the slope of the upper surface) and over the lower surface of any profile (provided that $-\tau\, h'(\xi)$ is the slope of the lower surface). Once the step from (12) to (14) has been made lifting and non-lifting effects can no longer be separated.

A wedge at incidence provides a simple example. The wedge at zero incidence has the equation $y = \tau x$ up to a point of discontinuity in slope. This point must be the sonic point; the slope of the profile after it is irrelevant. From (18),

$$u = \left(\frac{3}{\pi}\right)^{1/3} \frac{\tau^{2/3}}{(\gamma+1)^{1/3}} \left(\log\frac{x}{x^*}\right)^{1/3}$$

a result which is shown in ref.7 to agree well with a more exact solution[11]. If the wedge is now assumed to be at an incidence α, the formula for u on the upper surface becomes, (since the slope of this surface is $\tau - \alpha$),

$$u = \left(\frac{3}{\pi}\right)^{1/3} \frac{(\tau-\alpha)^{2/3}}{(\gamma+1)^{1/3}} \left(\log\frac{x}{x^*}\right)^{1/3} .$$

For the lower surface the sign in front of α must be changed. This result is obtained so simply and is so plausible that the complete lack of agreement with the known solution[13] is saddening. The reason is simply that the method used in this note does not allow for interference between the upper and lower surfaces; since the flow is subsonic over both surfaces, interference between them must occur. On the other hand, in the flow over a flat plate at a

positive incidence the flow over the upper surface is supersonic everywhere. The slope of the lower surface is α, where α is the incidence of the plate and so, on the lower surface,

$$u = \left(\frac{3}{\pi}\right)^{1/3} \frac{\alpha^{2/3}}{(\gamma+1)^{1/3}} \left(\log \frac{x}{x^*}\right)^{1/3} .$$

This result is a close approximation to the known solution[14], the small difference arising because there is a certain amount of spillage at the leading edge. The flow over the upper surface cannot be obtained by the present method, since u' is always negative there. These results suggest that, if the interference between upper and lower surfaces is small, then the present method works satisfactorily. Since the part of the profile where the flow is subsonic extends to only a very small percentage of the chord for some round-nosed profiles, it seems likely, therefore, that the method can be applied to such profiles at incidence. As stated in section 3, profiles for which this is not true are of little importance.

The technique can be illustrated by considering the profile defined by (19) at a positive incidence α. The slope of the lower surface is then given by

$$\tau\, h'(x) = \tfrac{1}{2}\tau \left[\left(\frac{c}{x}\right)^{\frac{1}{2}} - 3\left(\frac{x}{c}\right)^{\frac{1}{2}}\right] + \alpha \qquad (24)$$

Hence,

$$\frac{d}{dx}\int_0^x \frac{h'(\xi)\, d\xi}{(x-\xi)^{\frac{1}{2}}} = -\frac{3\pi}{4c^{\frac{1}{2}}} + \frac{\alpha}{\tau x^{\frac{1}{2}}} ,$$

so that (15) now provides a value for x^*, the sonic point on the lower surface

$$x^* = \frac{16}{9\pi^2}\left(\frac{\alpha}{\tau}\right)^2 c . \qquad (25)$$

At zero incidence $x^* = 0$ as was stated without proof in section 3; as α increases so does x^*, in agreement with experimental results[8]. (18) now gives, for the lower surface

$$u = \left(\frac{3}{\pi}\right)^{1/3} \frac{\tau^{2/3}}{(\gamma+1)^{1/3}} \left[\frac{9\pi^2}{16}\left(\frac{x}{c}\right) - 3\pi\left(\frac{\alpha}{\tau}\right)\left(\frac{x}{c}\right)^{1/2} + 3\left(\frac{\alpha}{\tau}\right)^2 + \right.$$

$$\left. + \left(\frac{\alpha}{\tau}\right)^2 \log\left\{\frac{9\pi^2}{16}\left(\frac{\tau}{\alpha}\right)^2 \frac{x}{c}\right\}\right]^{1/3} .$$

is some difficulty in obtaining a value for x^* on the upper surface. gives the formula

$$(x^*)^{\frac{1}{2}} = -\frac{4}{3\pi}\left(\frac{\alpha}{\tau}\right) c^{\frac{1}{2}} \quad , \qquad (26)$$

and the solution of this is again given by (25). The presence of the minus sign in (26) is, however, a little peculiar; in addition, (25) leads to the conclusion that the sonic point moves backwards as the incidence increases, which is contrary to experimental results[8]. Hence, it is proposed to put $x^* = 0$ on the upper surface for all positive incidences; since the sonic point is known[8] to move towards the leading edge with increasing incidence it seems unlikely that this approximation will provide results less satisfactory than those obtained for zero incidence. Hence, on the upper surface, neglecting terms of order $(\alpha/\tau)^2$

$$u = \left(\frac{3}{\pi}\right)^{1/3} \frac{\tau^{2/3}}{(\gamma+1)^{1/3}} \left[\frac{9\pi^2}{16}\left(\frac{x}{c}\right) + 3\pi\left(\frac{\alpha}{\tau}\right)\left(\frac{x}{c}\right)^{\frac{1}{2}} \right] .$$

For an arbitrary round-nosed profile the technique can be summarised as follows. For the lower surface, $h'(\xi)$ in (18) is to be replaced by $h'(\xi) + \left(\frac{\alpha}{\tau}\right)$, as in (24), while x^* is the solution of (15) with this modified form of $h'(\xi)$ inserted. For the upper surface $h'(\xi)$ in (18) is to be replaced by $h'(\xi) - \left(\frac{\alpha}{\tau}\right)$, while x^* is taken to be zero.

The technique has been applied to the profile of (22) at various incidences (0.5°, 1.0° and 1.5°), and the results ($\frac{p}{p_o}$ against $\frac{x}{c}$) are shown in Figs.4 to 9, (full lines). The curves are drawn up to $\frac{x}{c} = 0.4$, except for the lower surface at 1.5° incidence. There the curve goes up to the crest (at $\frac{x}{c} = 0.52$); in the other figures the crest occurs before $\frac{x}{c} = 0.4$. The dashed curves come from using Sinnott's method[10], described in the previous section. Some of the experimental results obtained by Holder and Cash[8] are also shown; the agreement is again reasonable. The figures show that $\alpha = 1.5^\circ$ has the least satisfactory agreement; calculations for higher incidences would probably be of little use.

5 DISCUSSION

As a result of the theoretical methods described in this note pressure distributions at sonic speed over the section NPL.491 have been satisfactorily predicted for a range of incidences (0° to 1.5°). Nevertheless, there are still many features of transonic flow over two-dimensional aerofoils which the present methods are unable to explain, and it is the purpose of this section to discuss these features.

The most satisfactory result of the present theory is that it is possible in many cases to predict the pressure distributions over both sharp-nosed and round-nosed profiles from a point near the leading edge to a point beyond the crest, with a knowledge of the aerofoil geometry only. The theory fails for sharp-nosed profiles at incidence and for round-nosed profiles the

equations of which contain terms in both $\left(\frac{x}{c}\right)^{\frac{1}{2}}$ and $\frac{x}{c}$ in an expansion about $\frac{x}{c} = 0$. It is difficult to envisage a simple extension (not empirical) of the theory to cover either of these two cases; neither case is of importance at the present time.

The method of Spreiter and Alksne[7] breaks down at the point on the profile where $\frac{du}{dx}$ becomes zero. Sinnott's method[10] has been used to extend the pressure distributions up to the trailing edge. This method makes use of an empirical result due to Holder[12], which enables the flow quantities at the trailing edge to be determined. That an empirical result must be used is a defect of the method described in this note; further work on the problem of extending the pressure distribution up to the trailing edge is planned.

The region close to the leading edge cannot be treated by the present method. For a symmetrical profile at zero incidence there is a stagnation point at the leading edge; the stagnation point is on the lower surface close to the leading edge for a symmetrical profile at a positive incidence. No "small disturbance" theory can be expected to apply in this region; (the present theory predicts an infinite pressure at the leading edge for a sharp-nosed profile, and sonic pressure for a round-nosed profile). The pressures are seriously in error in a small region only; at the point $\frac{x}{c} = 0.05$ the theoretical predictions are already in agreement with experimental results.

The present method gives incorrect results in the region of the trailing edge also. Examination of Figs.3 to 9 shows that, in general, the experimental pressures begin to fall near the trailing edge while the theoretical results continue to increase steadily. This is due to the slightly blunt trailing edge, which was ignored in the calculations.

The above discussion deals with flows at Mach number one only. It was stated in section 2 that the pressure distribution at a Mach number different from one can be obtained theoretically from the distribution at sonic speed because of the existence of the "Mach number freeze". Since $\frac{p}{p_o}$ can be expressed as a function of local Mach number alone, (i.e. the free stream Mach number does not explicitly appear in the relation connecting $\frac{p}{p_o}$ and local Mach number), it follows that the theoretical curves in Figs.3 to 9 are the same for Mach numbers other than one. This is not in good agreement with the experimental results. Because the open area of the slotted walls used in the experiments of Ref.8 was too large for interference-free flow in two-dimensional tests, the "Mach number freeze" would, however, be expected to be less pronounced than in free air.

There remains the problem of determining the position and strength of shocks on the profile. In general a shock first appears at a free stream Mach number just above the critical Mach number; as the free stream Mach number is increased the shock moves back and, at sonic speed, it is at (or

very near) the trailing edge. The present theory apparently offers no possibility of predicting either the position or the strength of a shock. This particular problem may well be very complicated; Holder and Cash[8] find that the increase in pressure across the shock is less than would be obtained by using the Rankine-Hugoniot relationships. It is possible that an inviscid theory is not sufficient to solve the problem.

This section has been largely a catalogue of unsolved problems, some of which present great difficulties, although they may perhaps be tractable by empirical methods. However, the pressure distributions over a large class of sharp-nosed and blunt-nosed profiles at sonic speed can now be predicted, and this is an advance on the position a year ago.

LIST OF SYMBOLS

c	aerofoil chord
c'	defined after equation (22)
$f(x,y)$	$(M_\infty^2-1)\,\phi_{xx} + [(\gamma+1)\,M_\infty^2\,\phi_{xx} - \lambda]\,\phi_x$
$g(x,y)$	written for $(\Delta\phi)_{\eta=0}$
h	defined by equation (3)
M_∞	free stream Mach number
p	static pressure
p_o	stagnation pressure
s	defined after equation (22)
t	$(x - x_m)/(c - x_m)$
U_∞	free stream speed
u	defined by equation (1a)
u_o	$u(x,0)$
v	defined by equation (1b)
x	Cartesian coordinate defined in section 2
x_m	position of crest of profile
x_o	point on profile at which flow quantities are given
x^*	position of sonic point on profile
y	Cartesian coordinate defined in section 2
α	incidence
γ	ratio of specific heats
$(\Delta\phi)_{\eta=0}$	defined by equation (9a)

LIST OF SYMBOLS (Contd.)

$\left(\Delta \frac{\partial \phi}{\partial \eta}\right)_{\eta=0}$	defined by equation (9b)
$\Delta\omega$	difference between true ω and simple wave ω
η	running coordinate corresponding to y
θ	defined after equation (22)
λ	arbitrary constant (see section 2)
ξ, ξ_1, ξ_2	running coordinates corresponding to x
σ	defined by equations (8a) and (8b)
τ	defined after equation (3)
ϕ	defined by equations (1a) and (1b)
ω	Prandtl-Meyer angle

Suffixes u and ℓ denote upper and lower surfaces respectively

Suffix t.e. denotes trailing edge

LIST OF REFERENCES

No.	Author	Title, etc.
1	Guderley, K.G.	Theorie Schallnaher Strömungen, Springer, 1957.
2	Oswatitsch, K.	Die Geschwindigkeitsverteilung bei Lokalen Überschallgebieten an flachen profilen, ZAMM, Vol.30, Jan/Feb, 1950, pp.17-24.
3	Gullstrand, T.K.	The flow over symmetrical profiles without incidence at sonic speed, KTH Aero TN.24, 1952.
4	Spreiter, J.R., Alksne, A.	Theoretical predictions of pressure distributions on non-lifting airfoils at high subsonic speeds. NACA Report 1217, 1955.
5	Behrbohm, H.	Näherungstheorie des unsymmetrischen Schalldurchgangs in einer Lavaldüse. ZAMM, vol.30, April 1950, pp.101-112.
6	Oswatitsch, K., Keune, F.	The flow around bodies of revolution at Mach number one. Proceedings of Conference on High Speed Aeronautics. Brooklyn, Jan.1955, pp.113-130.
7	Spreiter, J.R., Alksne, A.Y.	Thin airfoil theory based on approximate solution of the transonic flow equation. NACA T.N.3970, May, 1957.

LIST OF REFERENCES (Contd.)

No.	Author	Title, etc.
8	Holder, D.W., Cash, R.F.	Experiments with a two-dimensional aerofoil designed to be free from turbulent boundary-layer separation at small angles of incidence for all Mach numbers. R & M 3100, August, 1957.
9	Kármán, Th. von	Section A of "General Theory of High Speed Aerodynamics". Ed. Sears, W.R./O.U.P. 1955.
10	Sinnott, C.S.	On the flow of a sonic stream past an aerofoil surface. J.Aero/Space Sciences, March, 1959.
11	Guderley, G., Yoshihara, H.	The flow over a wedge profile at Mach number 1. Journal of Aeronautical Sciences, Vol.17, Nov. 1950, pp.723-735.
12	Holder, D.W.	Note on the flow near the tail of a two-dimensional aerofoil moving at a free stream Mach number close to unity. C.P.188, June, 1954.
13	Guderley, G., Yoshihara, H.	Two-dimensional unsymmetric flow patterns at Mach number 1. Journal of the Aeronautical Sciences, Vol.20, Nov., 1953, pp.757-768.
14	Guderley, G.	The flow over a flat plate with a small angle of attack at Mach number 1. Journal of the Aeronautical Sciences, Vol.21, April, 1954, pp.261-274.

WT.2078.C.P.456.K3 - Printed in Great Britain

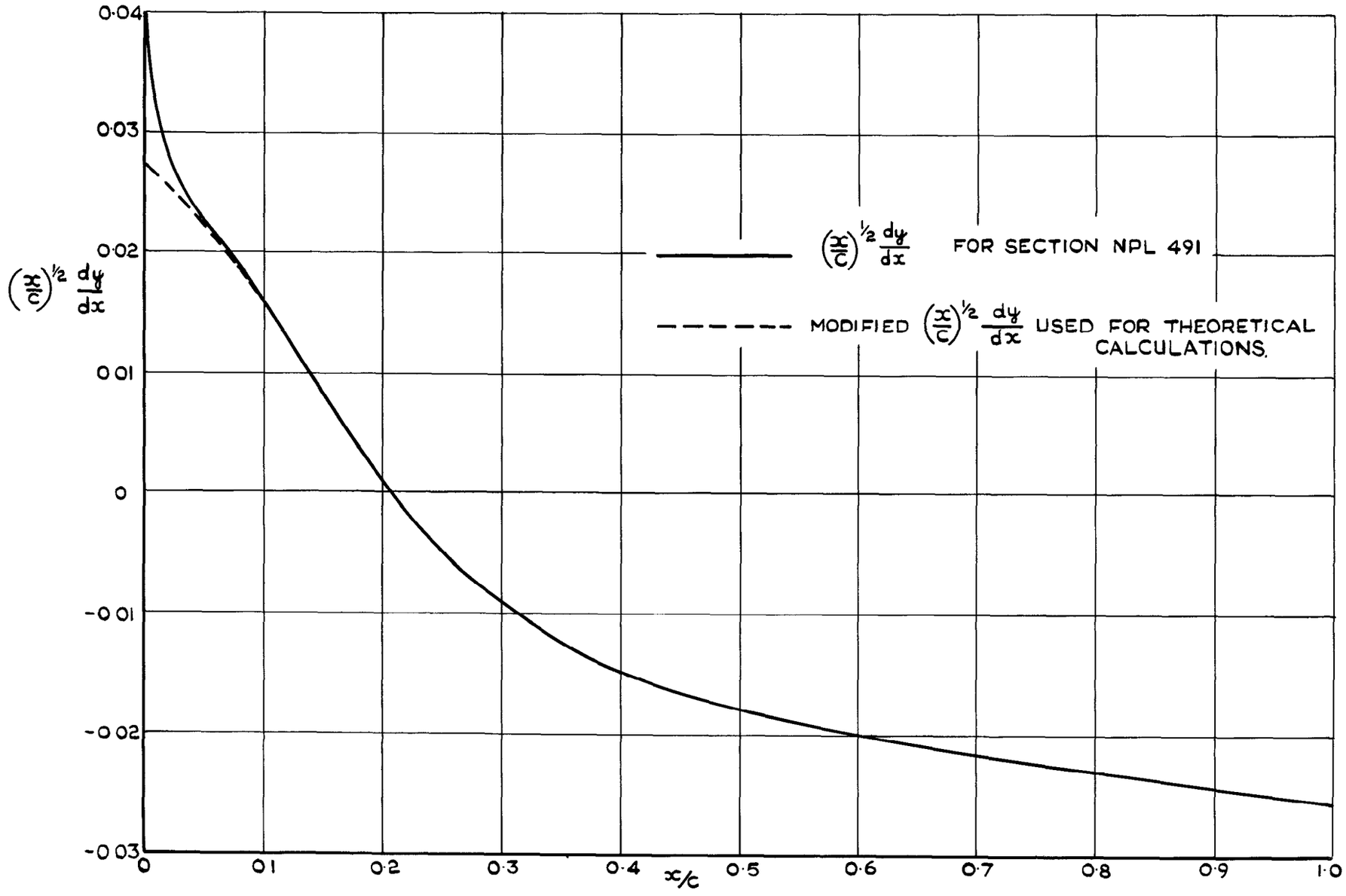

FIG. 1. SLOPE OF AEROFOIL SECTION NPL 491.

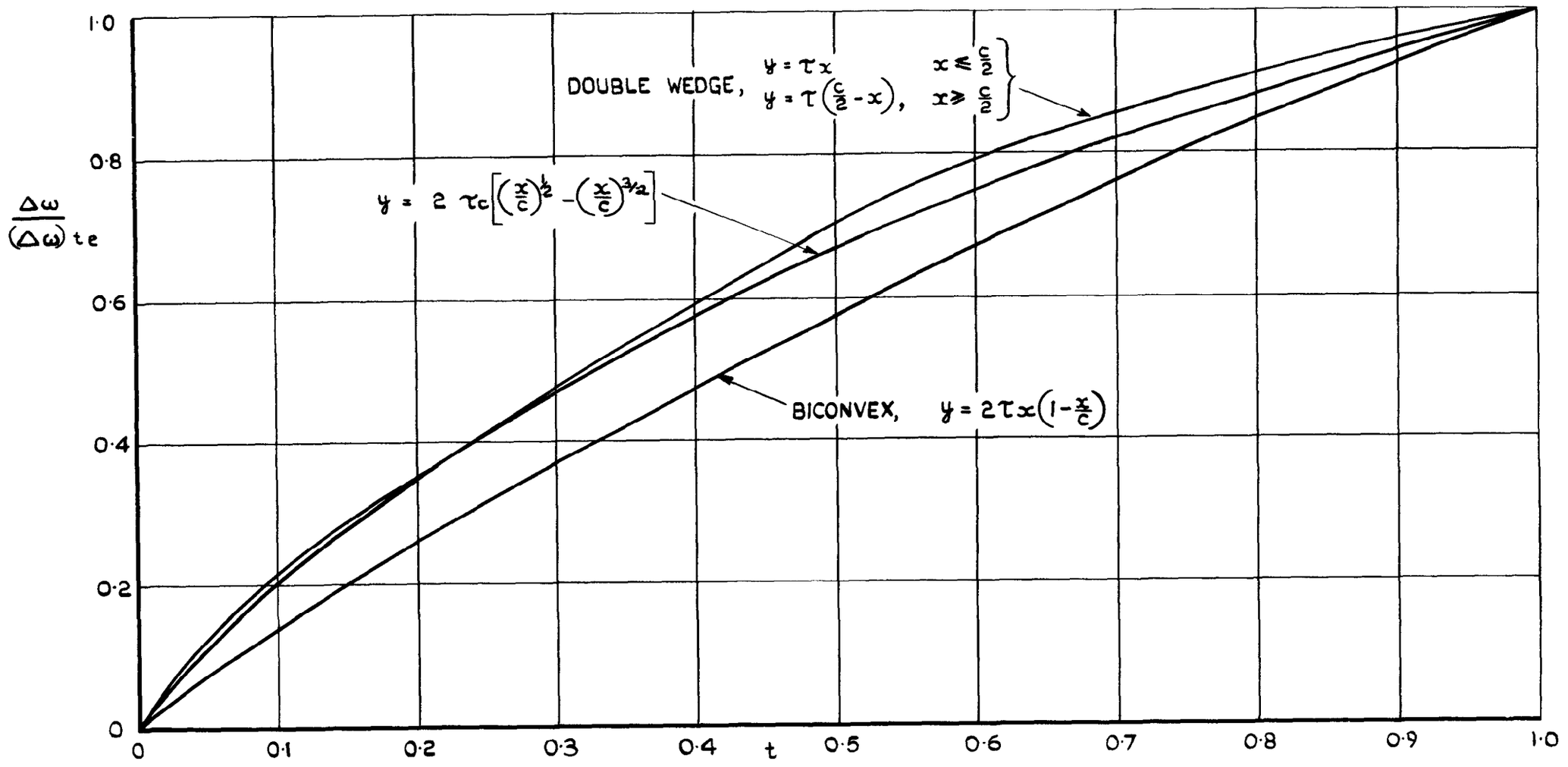

FIG. 2. ERROR IN ω CAUSED BY USING SIMPLE WAVE THEORY DOWNSTREAM OF CREST.
(THIS DIAGRAM IS EXPLAINED IN SECTION 3)

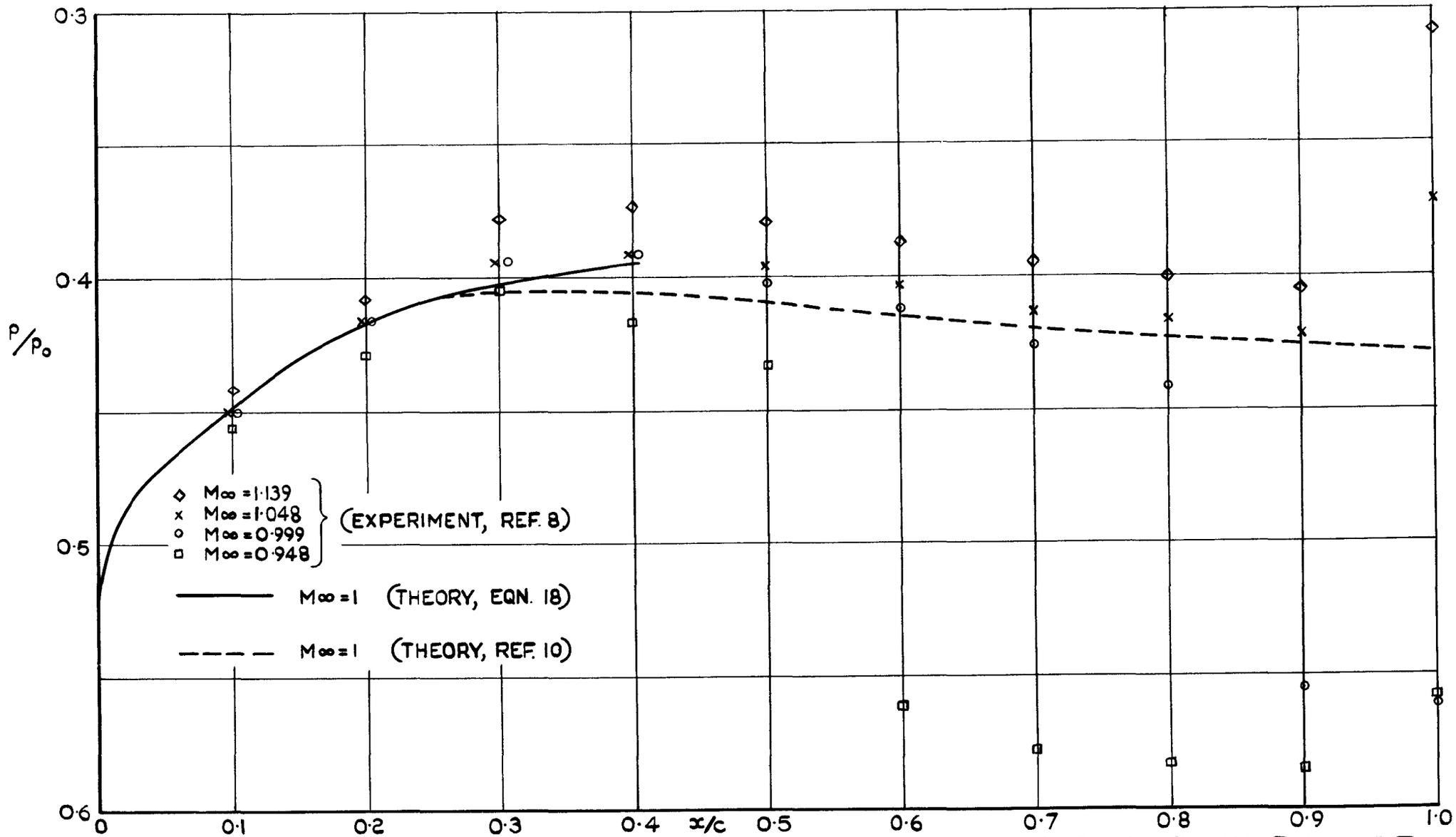

FIG. 3. THEORETICAL AND EXPERIMENTAL TRANSONIC PRESSURE DISTRIBUTIONS ON THE SECTION NPL 491. ZERO INCIDENCE.
(p_0 = STAGNATION PRESSURE)

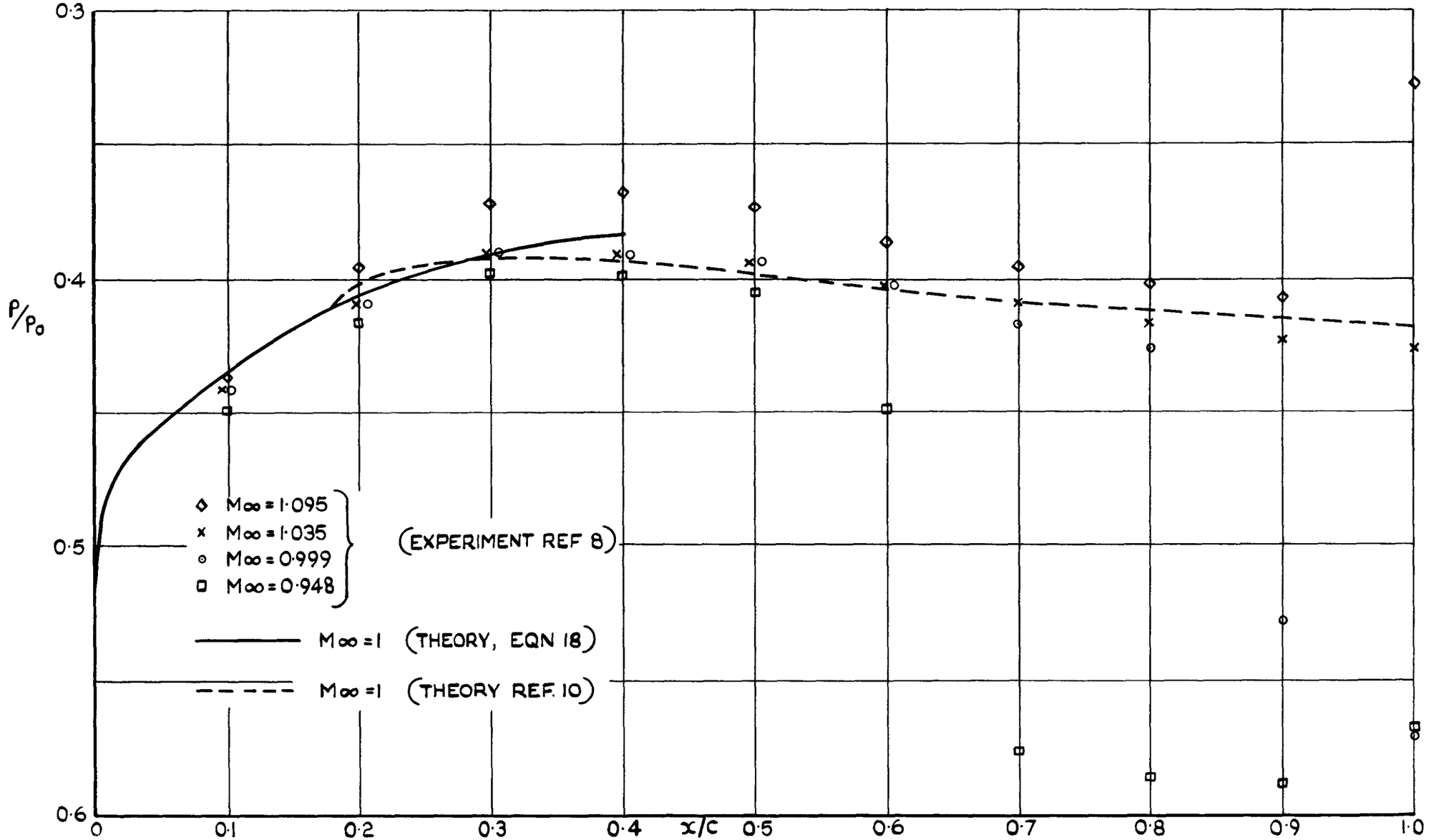

FIG. 4. THEORETICAL AND EXPERIMENTAL TRANSONIC PRESSURE DISTRIBUTIONS ON THE SECTION NPL 491. 0·5° INCIDENCE, UPPER SURFACE.
(p_0 = STAGNATION PRESSURE)

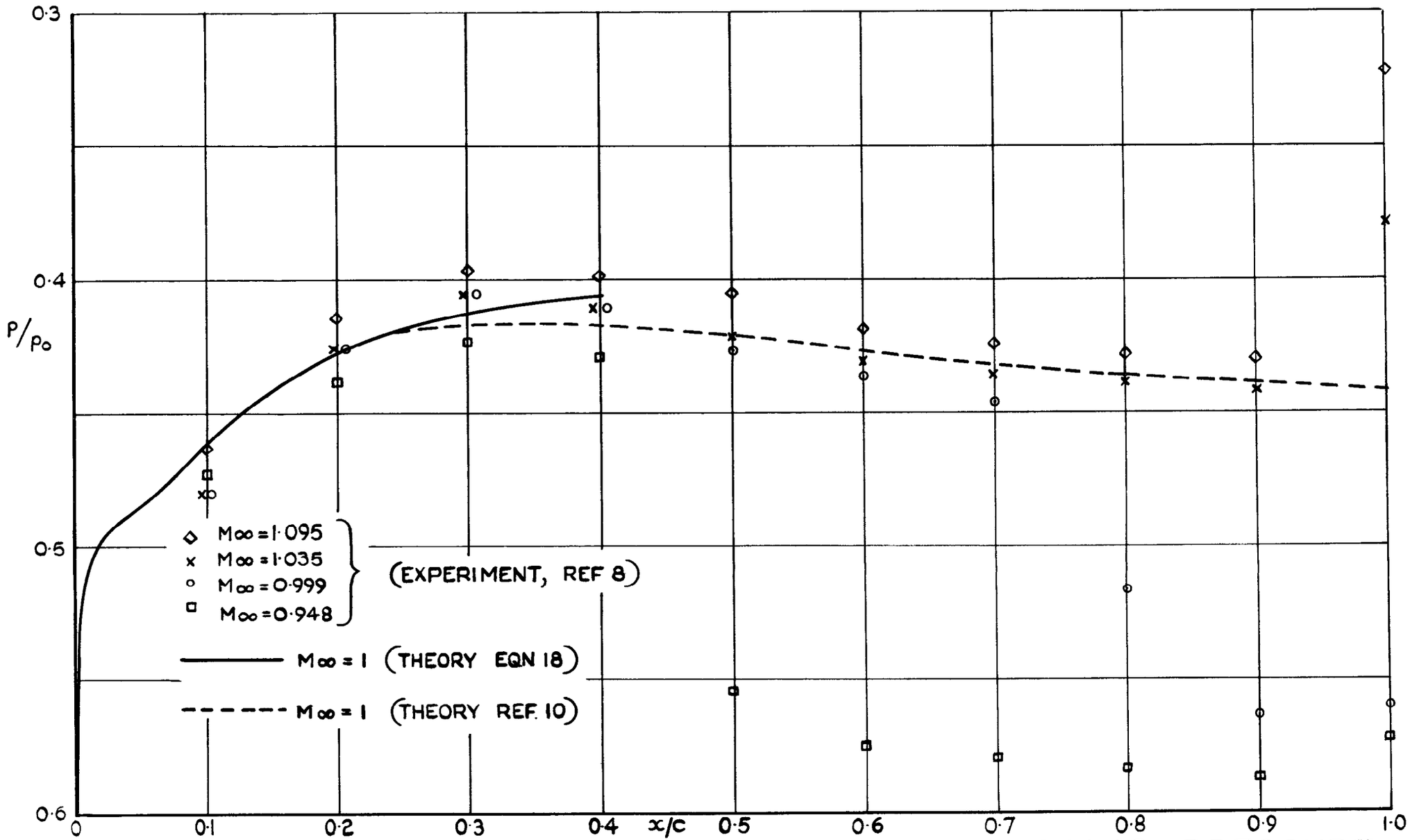

FIG. 5. THEORETICAL AND EXPERIMENTAL TRANSONIC PRESSURE DISTRIBUTIONS ON THE SECTION NPL 491. 0·5° INCIDENCE, LOWER SURFACE.
(P_0 = STAGNATION PRESSURE)

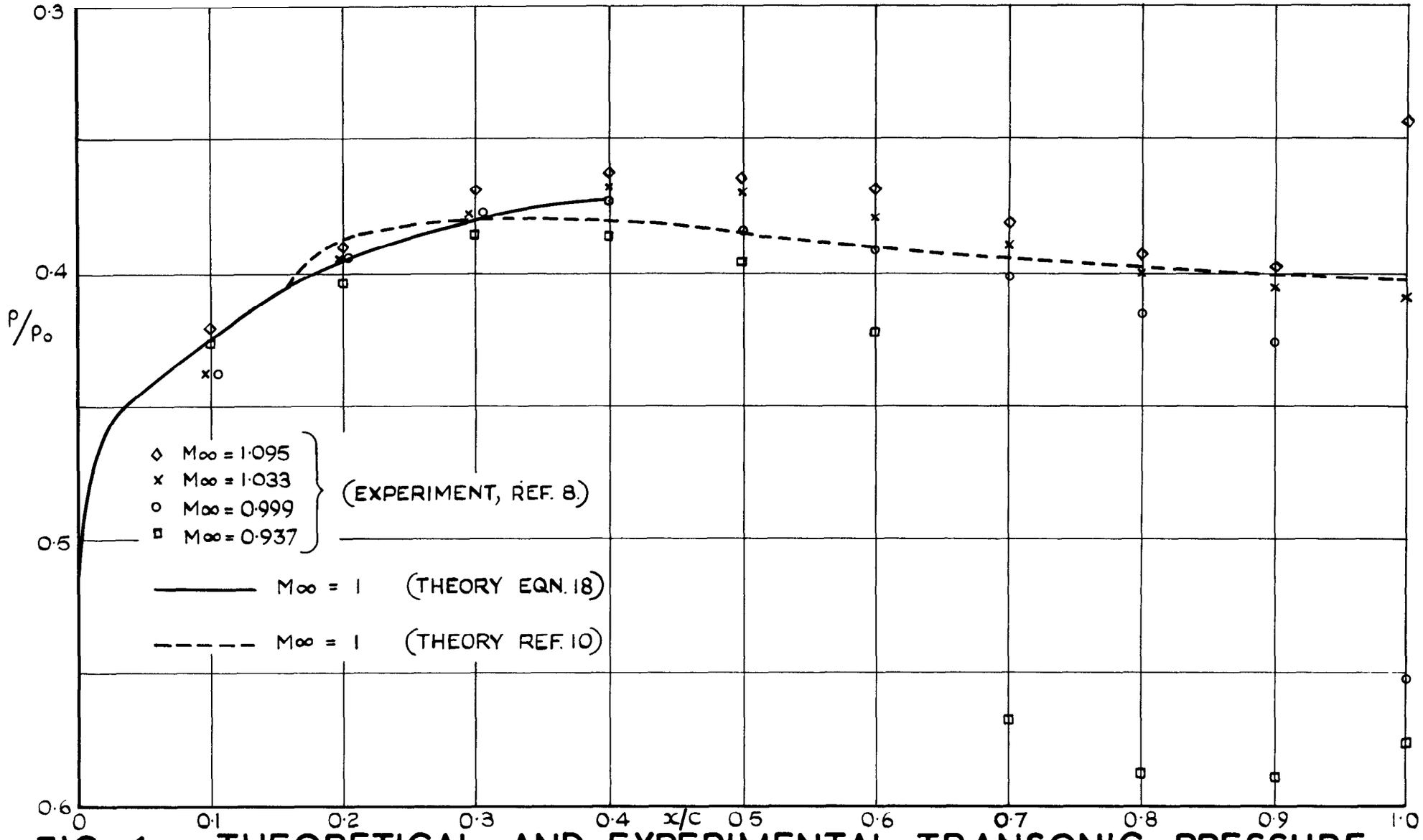

FIG. 6. THEORETICAL AND EXPERIMENTAL TRANSONIC PRESSURE DISTRIBUTIONS ON THE SECTION NPL 491. 1° INCIDENCE, UPPER SURFACE.
(p_0 = STAGNATION PRESSURE)

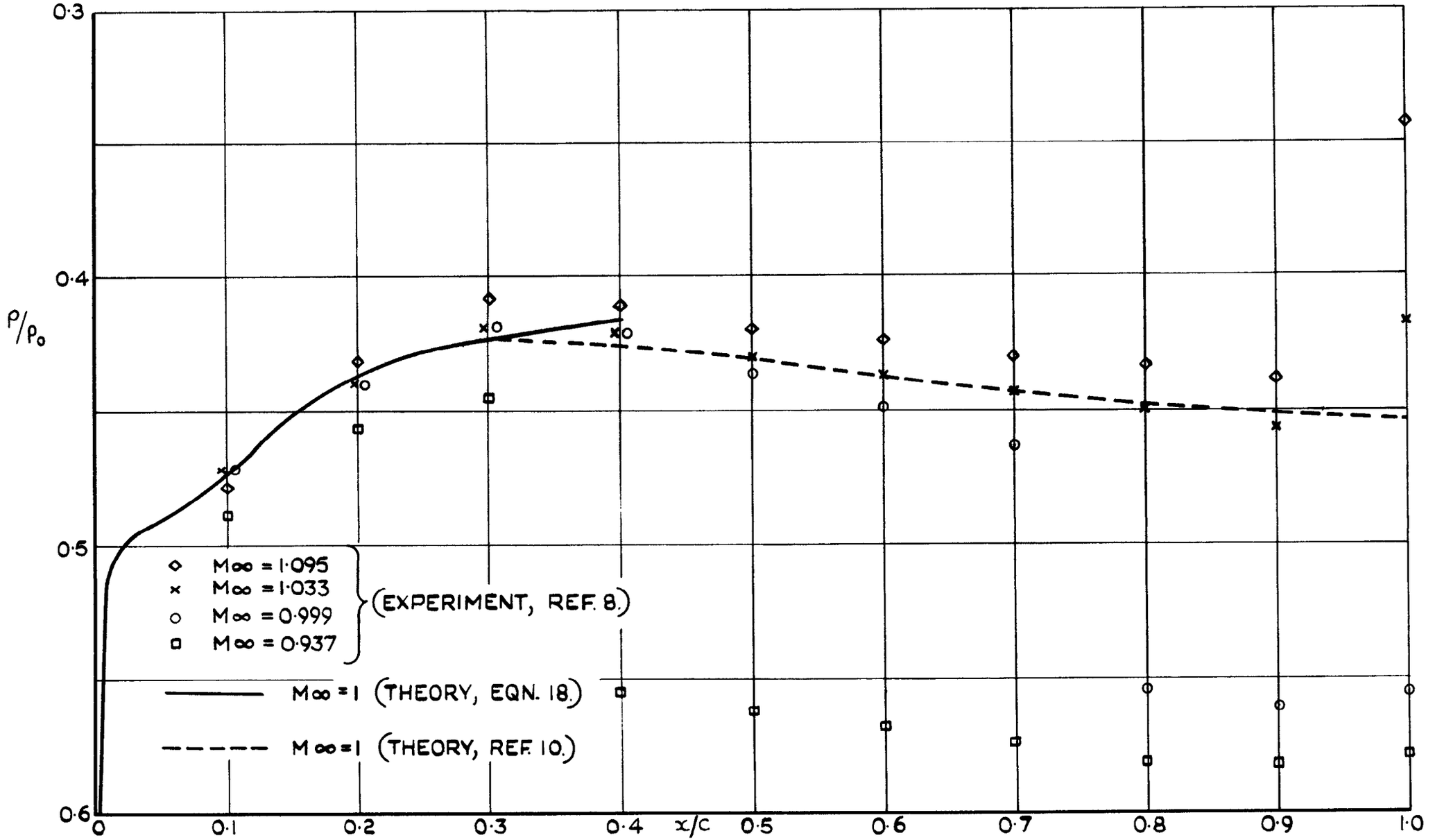

FIG. 7. THEORETICAL AND EXPERIMENTAL TRANSONIC PRESSURE DISTRIBUTIONS ON THE SECTION NPL 491. 1° INCIDENCE, LOWER SURFACE

(p_0 = STAGNATION PRESSURE)

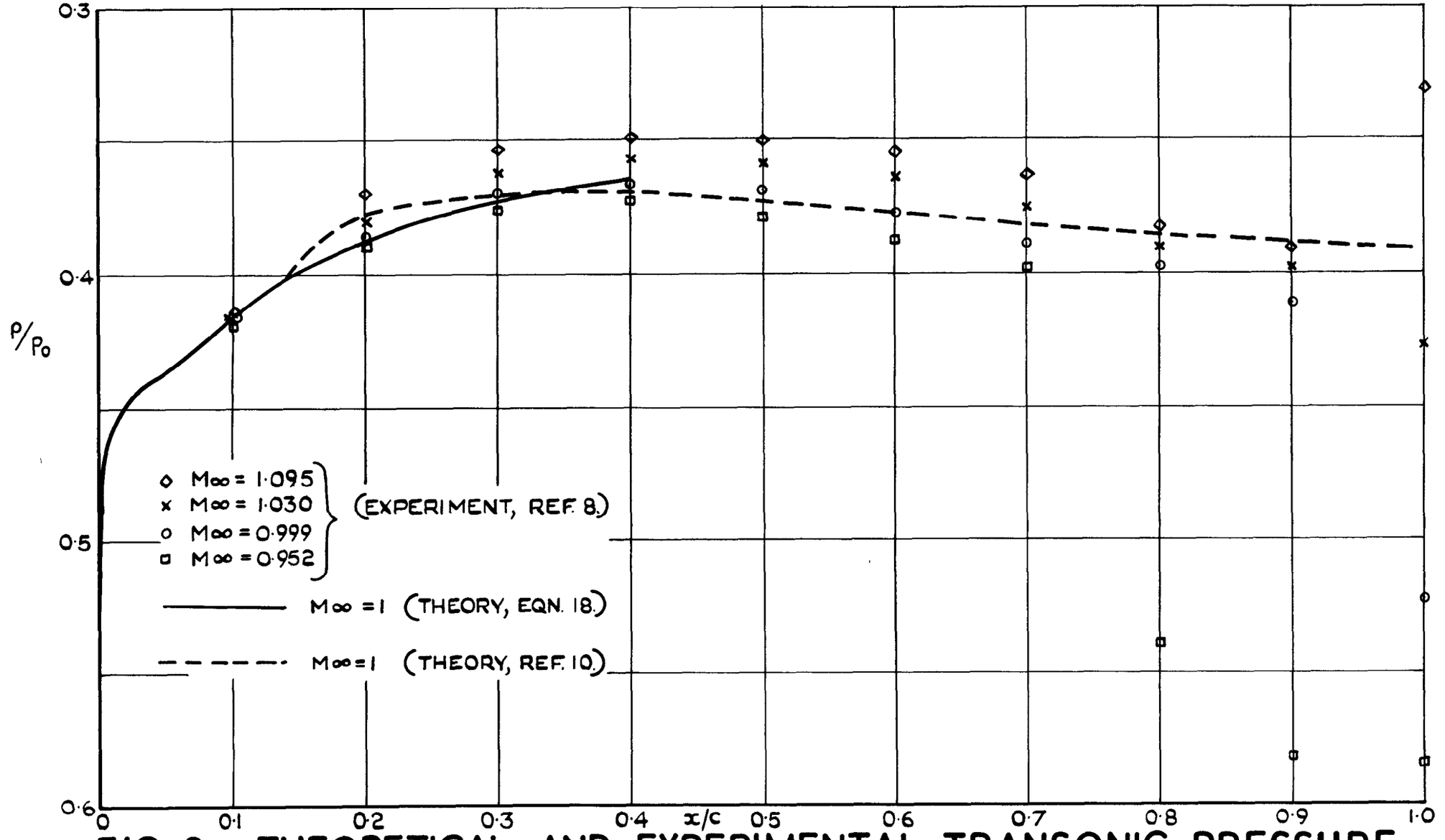

FIG. 8. THEORETICAL AND EXPERIMENTAL TRANSONIC PRESSURE DISTRIBUTIONS ON THE SECTION NPL 491. 1·5° INCIDENCE, UPPER SURFACE.
(p_0 = STAGNATION PRESSURE)

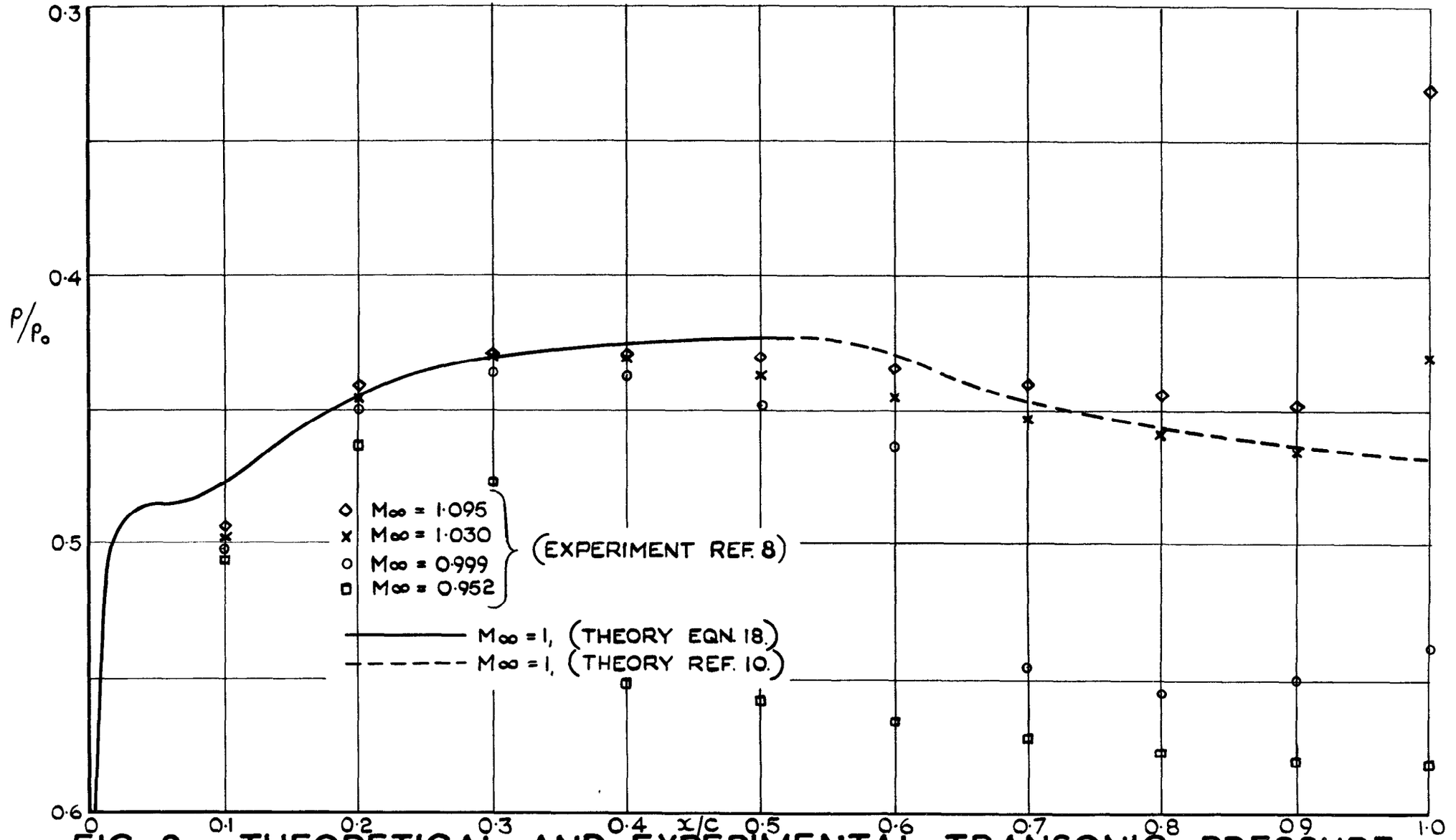

FIG. 9. THEORETICAL AND EXPERIMENTAL TRANSONIC PRESSURE DISTRIBUTIONS ON THE SECTION NPL 491. 1·5° INCIDENCE, LOWER SURFACE.
(p_0 = STAGNATION PRESSURE)

C.P. No. 456
(20,677)
A.R.C. Technical Report

Published by
HER MAJESTY'S STATIONERY OFFICE

To be purchased from
York House, Kingsway, London w.c.2
423 Oxford Street, London w.1
13A Castle Street, Edinburgh 2
109 St. Mary Street, Cardiff
39 King Street, Manchester 2
Tower Lane, Bristol 1
2 Edmund Street, Birmingham 3
80 Chichester Street, Belfast
or through any bookseller

Printed in Great Britain

S.O. Code No. 23-9011-56
C.P. No. 456